Indian Journal of Chemical Technology
Vol. 29, May 2022, pp. 251-260

Removal of Erythrosine B using *Prosopisspicigera L.* wood carbon-iron oxide composite

R Dhana Ramalakshmi*[,1] , M Murugan[2] &V Jeyabal[3]

[1]Department of Chemistry, Rani Anna Government College for Women, Tirunelveli 627 008, Tamil Nadu, India.

[2]Department of Chemistry, Sri K.G.S. Arts College, Srivaikuntam 628 619, Thoothukudi, Tamil Nadu, India.

[3]Department of Chemistry, St. Xavier's College (Autonomous), Palayamkottai, Tirunelveli 627 002, Affiliated to Manonmaniam Sundaranar University, Abishekapatti, Tirunelveli 627 012, Tamil Nadu, India.

E-mail: dhana.ram11@gmail.com

Received 15 August 2021; accepted 4 March 2022

The present study investigates the removal of Erythrosine B (EB), a neurotoxin and carcinogenic dye from aqueous system using *Prosopisspicigera L.* wood (PsLw) carbon-iron oxide composite. The adsorbent is well characterized by Fourier Transform Infra Red spectroscopy (FTIR), Scanning Electron Microscope (SEM) for surface morphology, Brunauer-Emmett-Teller nitrogen adsorption method (BET)/methylene blue method for surface area determination and potentiometric methods for surface charge (pH_{zpc}) determination. The removal capacity of the adsorbent has been evaluated by batch method under varying *p*H, contact time, adsorbate initial concentrations, and in the presence of other ions. The Langmuir maximum adsorption capacity is found to be 487.8 mg/g at *p*H = 2.0 for an initial concentration of 250 mg/L. The adsorption follows pseudo second order kinetics and fits to Langmuir isotherm. The adsorption is thermodynamically spontaneous and exothermic in nature. Pore diffusion and mass transfer studies are performed. Column mode analysis is applied in the process for industrial applications.

Keywords: Adsorption, Erythrosine B, Isotherm, Kinetics, *Prosopisspicigera L.* wood carbon-iron oxide composite, Thomas model

Erythrosine B is an anionic water soluble xanthane family dye, which is used as food colouring, printing, biological stain and mainly used as colorant in drugs, cosmetics and textile industry. The effluents of these industries contain remarkable amount of erythrosine, causes chronic problems of cancer and thyroid tumour. It affects the function of thyroid gland due to the presence of iodine in the dye and it is released during degradation. It can be one of the causes of atopic diseases[1]. The toxic and carcinogenic behaviour of erythrosine attracted global attention for its removal from waste water. Removal of EB from aqueous solution is a challenging task, due to its high solubility in water and possibility of generation of toxic intermediates during the course of process. Many physical, chemical and biological methods are available for dye removal. Photo catalytic degradation and biodegradation of dye have some metabolic intermediates after degradation and are more toxic. Therefore, adsorption technique is still economic, easy to operate and highly efficient without any harmful effects. Among various adsorbents, activated carbon is one of the most effective adsorption but the application of activated carbon in waste water treatment is limited due to the difficulty in separation, reuse of the adsorbent and high cost. The preparation of magnetic composites based on activated carbon and iron oxide is one of the methods to overcome the above limitation[2-5]. The magnetic composite based activated carbon provides high surface area, high adsorption efficiency and regeneration capacity. In the present work, attempts have been made to prepare a low cost adsorbent from *Prosopisspicigera L.* wood carbon and iron oxide for the removal of EB from aqueous solution.

Experimental Section

Materials

PsLw carbon-iron oxide composite preparation

PsLw plant material used in the present work was collected from the dry land area of Palayamkottai in

Tirunelveli district, Tamilnadu state, India. The branch and roots of the plant were cut into pieces and piled up on a firing hearth. Before firing, the heaped wood pieces were enclosed by fresh plantain pith and the whole mass was covered and plastered with layers of wet clay. This arrangement prevented the direct entry of air into wood pieces and hence prohibited burning of wood and its becoming ash. After 48 h of continuous firing and subsequent natural cooling, the activated carbon was obtained. After removing the non-carbonaceous materials the carbon was isolated, crushed and sieved to 75 micron particles. The composite adsorbent was prepared using the slightly modified literature procedure[6,7]. 20 g of PsLw carbon was suspended in 400 ml of $FeCl_3$ (7.8 g, 28 mmol) and $FeSO_4$ (3.9 g, 14 mmol) at 70°C. The above solution was stirred well using a magnetic stirrer for 3 h. Sodium hydroxide solution (100 mL, 5 mol/L) was added dropwise to precipitate the iron oxides. Again the stirring was continued for another two hours at 70°C. Later the solid material was separated, washed with de-ionised water until the washings become neutral. Further the washings were tested for iron with 1:10 phenanthroline for reddish colour or precipitates. The final product was dried in an air oven at 100°C for 8 h and finally stored in air tight containers.

Characterisation of the adsorbent

The surface morphology of PsLw carbon-iron oxide composite was analysed on Jeol, JSM 6390, Oxford instruments, UK, Scanning Electron Microscope (SEM). Fourier Transform Infra Red (FTIR) spectroscopy was studied on JASCO FT/IR-4700 type A, to analyse the surface functional groups. The zero point charge of the adsorbent was investigated by potentiometric titration[6]. The surface area of the adsorbent was identified by methylene blue method[8-10] and Nitrogen BET adsorption method.

Batch equilibrium studies

Standard Erythrosine B stock solution of 1000 mg/L was prepared by dissolving 1 g of Erythrosine B with 1000 mL of deionized water. This stock solution was utilized for batch studies. Batch equilibrium studies were carried out for adsorption of dye on PsLw carbon- iron oxide composite. The effect of *p*H, initial concentration, contact time, in the presence of other ions and solution temperature of the adsorbate solution on PsLw carbon-iron oxide composite were studied. The sample solutions were analysed at particular time intervals by measuring absorbance at 533 nm using UV-Vis spectrophotometer (Shimadzu, AA-6300). The concentration of the solution was determined from a standard plot using linear regression equation.

The amount of adsorbate adsorbed at equilibrium, q_e(mg/g) is calculated using the equation

$$q_e = (C_\circ - C_e)V/W \quad \ldots(1)$$

where, C_o and C_e (mg/L) are the initial and equilibrium concentration of adsorbate respectively. V is the volume of the solution (L) and W is the mass of adsorbent (g).

Adsorption Isotherm models

Equilibrium adsorption isotherm expresses the relationship between the surface of the adsorbent and the adsorbate molecule and adsorption efficiency of dye under different conditions. The linear form of Langmuir and Freundlich models can be expressed as

$$C_e/q_e = 1/Q_\circ b + C_e/Q_\circ \quad \ldots(2)$$

$$\log q_e = \log K_f + 1/n \log C_e \quad \ldots(3)$$

where, C_e and q_e are the free and sorbed concentration of dye species respectively at equilibrium (mg/g), Q_o is the monolayer sorption capacity and b is the Langmuir adsorption equilibrium constant (L/mg). K_f (mg/g) and 1/n are the Freundlich constants related to the adsorption capacity and heterogeneity respectively.

Adsorption kinetics

The kinetics of the adsorption EB dye on PsLw carbon-iron oxide composite are described using pseudo first and the second order models at different concentrations and temperatures. The pseudo first order rate equation of Lagergren is expressed as

$$\log(q_e - q) = \log q_e - k_1 t/2.303 \quad \ldots(4)$$

where, q_e and q are the amounts of dye adsorbed at equilibrium and at a time 't' and k_1 is the rate constant for first order adsorption. The pseudo second order Ritchie kinetic rate equation can be written as

$$t/q = (1/k_2 q_e^{\,2}{}_{(cal)}) + t/q_{e(cal)} \quad \ldots(5)$$

where, k_2 is the reaction rate constant of second order adsorption and $q_{e\,(cal)}$ is numerically determined parameter.

Column study

The experimental unit consists of a glass column of 48 cm height by 3.5 cm diameter packed with 5 g of PsLw carbon-iron oxide composite. The column was fitted with cotton screens to separate the adsorbent from the top and bottom stoppers. The EB dye solution was drawn into the column from a height of 1 meter. Elutents were collected at regular interval of time and analysed. The data were analysed using Thomas model[11,12], which is given by the equation.

$$\log\left(C_\circ/C_e - 1\right) = kq_\circ M/Q - kC_\circ V/Q \qquad \ldots(6)$$

where, C_o and C_e are the influent and effluent EB dye concentrations (mg/L) respectively, K is the Thomas rate constant (mL/min/mg), q_o is the maximum solid phase concentration of solute (mg/g), M is the mass of the adsorbent (g), Q is the influent flow rate (mL/min) and V is the through put volume (mL/min).

Results and Discussion

Characterisation of the adsorbent

The physico-chemical characteristics of PsLw carbon-iron oxide composite are listed in Table 1.

FTIR spectra

The FTIR spectrum is the most useful physical method used for identifying functional groups and knowing the adsorption of adsorbate molecule on the adsorbent surface. The FTIR spectra of pure PsLw carbon, PsLw carbon-iron oxide composite and EB loaded PsLw carbon-iron oxide composite are illustrated in Figs 1(a), (b) and (c) respectively. The free PsLw carbon shows three weakly intense peaks at 1613 cm^{-1} (due to ketone moiety), 1423 cm^{-1} (O-H in plane bending) and 961 cm^{-1} (C-O stretching) [Fig. 1(a)]. The weak bands of PsLw carbon disappeared and shifted due to the modification of surface with iron oxide [Fig. 1(b)]. The EB dye loaded adsorbent Fig. 1(c) exhibits a band at 3426 cm^{-1} due to the presence of O-H stretching which indicates the material contains hydroxyl groups. The adsorption peak at 2916 cm^{-1} is assigned to O-H stretching vibration of carboxylic group (-COOH). The adsorption peak at 1747 cm^{-1} can be assigned to C=O stretching vibration (carbonyl group) and 1450 cm^{-1} implies O-H bending mode of vibration. The weak band at 876 and 697 cm^{-1} indicate the C-I stretching vibrations of the EB dye[16]. These changes confirm the adsorption of EB dye on the PsLw carbon-iron oxide composite surface.

Table 1 — Physico-chemical characteristics of PsLw carbon-iron oxide composite

Parameters	Value
*p*H	7.1
Moisture Content % (W/W)	0.0123
Surface area (m^2/g) (Nitrogen BET adsorption method)	120.91
Surface area (m^2/g) (Methylene Blue dye adsorption method)	64.53
pH_{zpc}	8.22
Bulk density (g/cc)	0.4137
Particle density (g/cc)	1.3790

SEM

SEM is a key tool for analysing the morphology of adsorbent surface. The SEM image of pure PsLw carbon have rough external surface with pores [Fig. 2(a)] and agglomerated with iron oxide particles [Fig. 2(b)]. EB dye entered into the pores of the adsorbent and the surface becomes darker with strong agglomeration [Fig. 2(c)]. Thus SEM images show the loading of EB dye on PsLw carbon-iron oxide composite.

Effect of *p*H

The *p*H of the solution exerts a strong influence of dye adsorption because *p*H may alter the surface charge of the adsorbent. The effect of *p*H on the adsorption of EB is shown in Fig. 3(a). The results show that the adsorption capacity decreases with increasing *p*H and maximum uptake for EB is 47.7 mg/g for an initial concentration of 25 mg/L at *p*H = 2.0. The pH_{zpc} value of PsLw carbon-iron oxide composite is 8.22 and the surface of the adsorbent is positively charged below *p*H = 8.22.

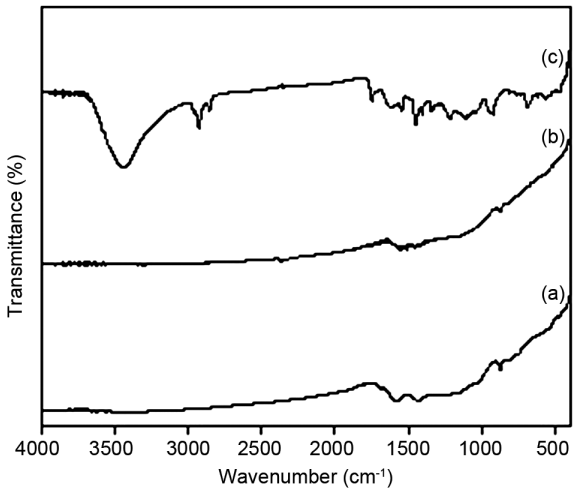

Fig. 1 — IR spectra of (a) pure PsLw carbon; (b) PsLw carbon-iron oxide composite and (c) EBloaded PsLw carbon-iron oxide composite.

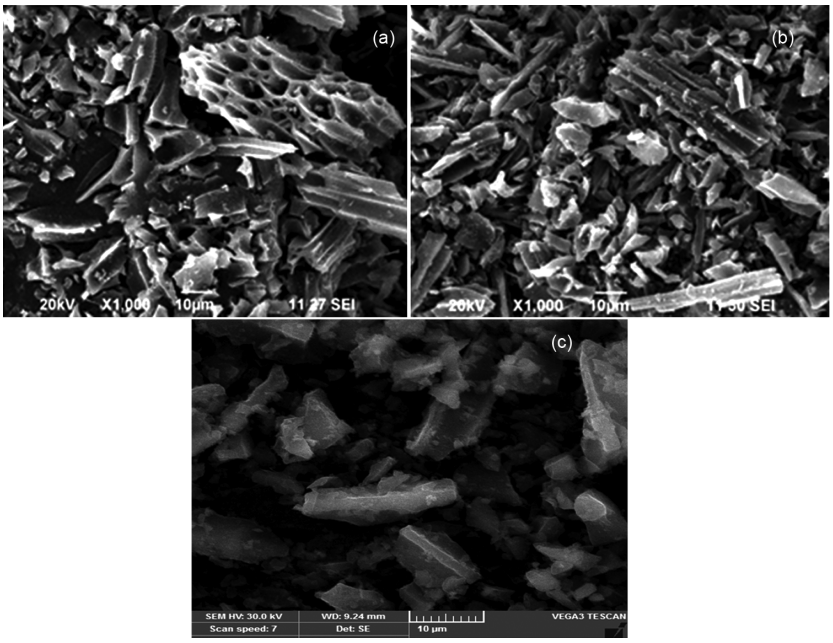

Fig. 2 — SEM images of (a) pure PsLw carbon; (b) PsLw carbon-iron oxide composite and (c) EB loaded PsLw carbon-iron oxide composite.

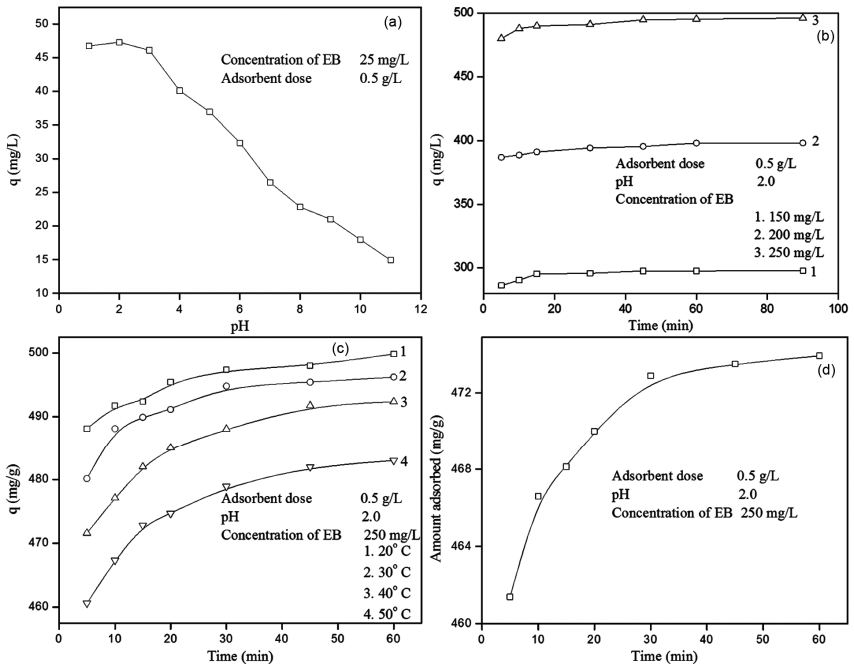

Fig. 3 — (a) Effect of pH on the adsorption of EB dye by PsLw carbon-iron oxide composite; (b) Effect of contact time and initial concentration on the removal of EB dye by PsLw carbon-iron oxide composite; (c) Effect of temperature on the removal of EB dye by PsLw carbon-iron oxide composite and (d) — Effect of EB dye removal by PsLw carbon-iron oxide composite in the presence of NO_3^-, Cl^-, SO_4^{2-} and CO_3^{2-} ions.

Hence an optimum *p*H = 2.0 is chosen for batch and kinetic studies[13,14].The high dye uptake efficiency at acidic *p*H arises due to the electrostatic attraction between the positively charged surface of adsorbent and negatively charged adsorbate[15]. This is evident from the FTIR spectral and SEM studies.

Effect of initial concentration and contact time

The effect of contact time and initial concentration of dye on the extent of removal of EB on PsLw carbon-iron oxide composite is shown in Fig. 3(b). Initially, the dye uptake capacity increases slowly upto 15 min and attain equilibrium after 60 min. The maximum adsorption capacity of EB dye at three different initial concentrations 150, 200, 250 mg/L is 299.8, 398.1 and 499.8 mg/g respectively.

Effect of temperature

The degree of adsorption depends on the temperature and the rate of adsorption was studied in the temperature range of 20-50°C. Figure 3(c) shows the effect of temperature on sorption process. The maximum dye adsorption of adsorbent is 499.8, 496.2, 492.3, 487.4 mg/g for 20, 30, 40, 50°C respectively with an initial concentration of 250 mg/L. The adsorption efficiency of PsLw carbon-iron oxide composite decreases with increasing temperature and the nature of adsorption process is exothermic[17].

Influence of the presence of other ions in adsorption

Batch adsorption study was carried out in the presence of other ions such as carbonate, nitrate, chloride and sulphate of concentration 0.001 M each shown in Fig. 3(d). The adsorption capacity increases with time and equilibrium is reached at 45 minutes for an initial concentration of 250 mg/L. The maximum adsorption capacity of EB dye was found to be 473.9 mg/g which is lower than the adsorption capacity of EB dye in the absence of other ions. This may be due to the competition between other ions with EB dye molecules for the same number of adsorption sites. This is helpful for the application of present study to practical applications.

Adsorption Isotherm

The adsorption isotherm was analysed by two well-known models of Freundlich and Langmuir isotherm models. Langmuir isotherm offers the monolayer coverage on homogeneous surface and Freundlich isotherm predicts heterogeneous surface.The linear plots of C_e/q against C_e in Langmuir model for the uptake of EB dye on PsLw carbon-iron oxide composite at different concentrations and temperatures is shown in Fig. 4 and the Langmuir parameters of Q_o and b can be calculated from the slope and intercept of the linear plots respectively. The Freundlich parameters of 1/n and K_f are determined from the slope and intercept of the linear plot of log q_e and log C_e respectively which is shown in Fig. 5. Table 2 summarises the Langmuir and Freundlich isotherm parameters. The experimental data show the maximum adsorption capacity of Langmuir model is 487.8 mg/g at 20°C for 250 mg/L initial concentration. From the results of isotherm, the adsorption of EB dye on PsLw carbon-iron oxide composite fits good to Langmuir model than Freundlich model.

The nature of adsorption isotherm can be determined by the separation factor $R_{L,}$ dimensionless constant, which is given as

$$R_L = 1/(1 + bC_\circ) \qquad \ldots(7)$$

where, C_o is the initial concentration (mg/L) of EB dye. R_L values were found to be positive and less than unity ($0<R_L<1$) denote the sorption of EB dye is favourable under the studied condition and the R_L values are listed in Table 2.

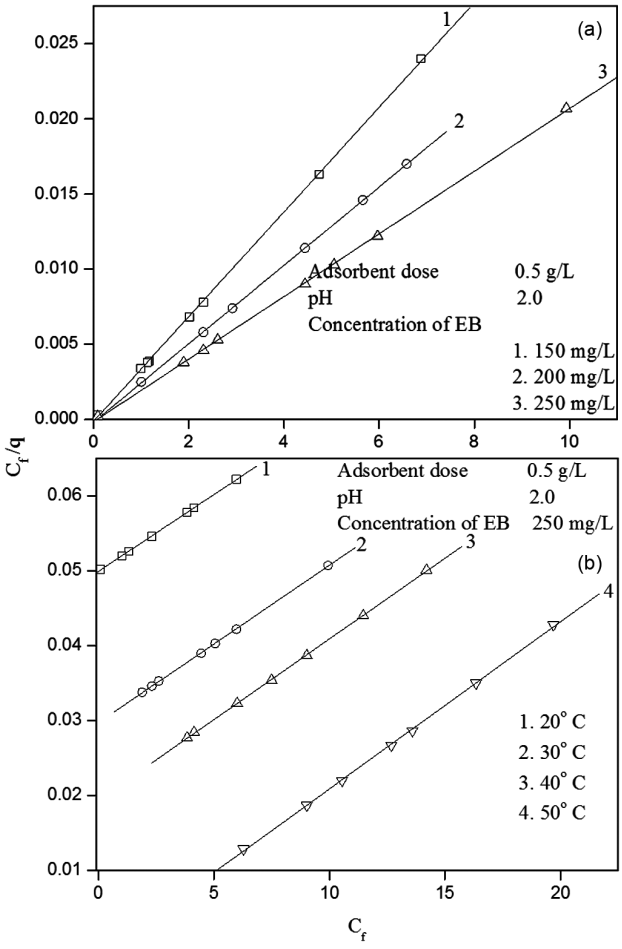

Fig. 4 —Langmuir isotherm for EB dye adsorption onto PsLw carbon-iron oxide composite at different (a) concentrations and (b) temperatures.

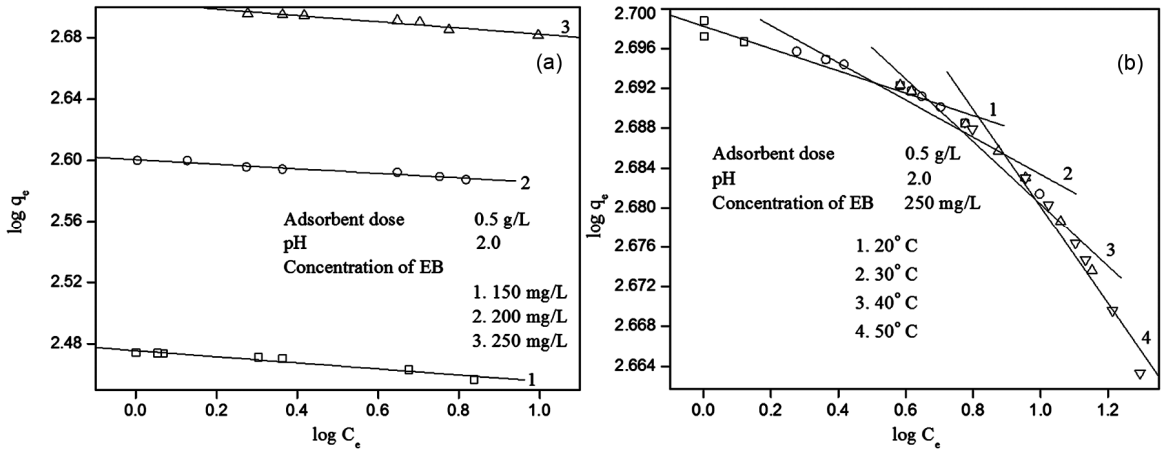

Fig. 5 — Freundlichisotherm for EB dye adsorption onto PsLw carbon-iron oxide composite at different (a) concentrations and (b) temperatures.

Table 2 —Langmuir and Freundlich constants at different concentrations and temperatures

		Langmuir Isotherm				Freundlich Isotherm		
C_o (mg/L)	Temp (°C)	Q_o (mg/g)	b (L/mg)	R_L	R^2	n	K_f (mg/g)	R^2
150	30	287.36	29.49	0.0002	0.9998	-50.4796	298.9096	0.9410
200	30	383.14	14.74	0.0003	0.9998	-67.6132	398.5749	0.9586
250	30	480.77	13.96	0.0002	0.9996	-79.2854	504.0060	0.9297
250	20	487.80	34.36	0.0012	0.9998	-89.2061	499.1602	0.9553
250	30	480.77	14.74	0.0062	0.9998	-79.2854	504.0806	0.9297
250	40	465.12	03.60	0.0011	0.9998	-31.7662	515.0151	0.9637
250	50	448.43	1.62	0.0025	0.9998	-20.4457	535.7967	0.9623

Table 3 — Comparison of pseudo-first order and pseudo-second order kinetic parameters

			Pseudo first order			Pseudo second order		
C_o (mg/L)	Temp (°C)	q_e(exp) (mg/g)	k_1 (min^{-1})	q_e(cal) (mg/g)	R^2	k_2 (g/mg/min)	q_e (cal) (mg/g)	R^2
150	30	299.82	0.0221	09.03	0.7600	0.0141	298.51	1
200	30	398.15	0.0206	09.44	0.8434	0.0087	400.0	0.9999
250	30	499.82	0.0183	15.02	0.8684	0.0065	500.0	0.9999
250	20	499.91	0.0285	11.22	0.8938	0.0100	500.0	0.9999
250	30	499.82	0.0372	16.36	0.8811	0.0065	500.0	0.9999
250	40	492.34	0.0388	27.66	0.9978	0.0056	495.05	0.9999
250	50	487.46	0.0399	29.12	0.9781	0.0040	490.20	0.9999

Adsorption kinetics

The adsorption kinetics is described by the Lagergren's pseudo-first order kinetic model[18]and Ritchie's pseudo-second order kinetic model[19] and is expressed by equations 4 and 5. From equation 4, a plot of log (q_e-q) against 't' gives a linear plot (plots are not shown). The values of k_1 and q_e are calculated from the slope and intercept of the plot respectively. The k_1 and q_e values are given in Table 3. Further from the pseudo-second order kinetic equation a linear plot is obtained by plotting 't/q_t' versus 't' (Fig. 6). The slope and the intercept of the equation gives q_e and k_2 respectively and are entered in Table 3. The kinetic parameters for the adsorption of EB shows, the pseudo-second order model is best followed than the pseudo-first order model under different initial concentration and temperatures.

The closeness of experimental ($q_{e(exp)}$) adsorption capacity obtained from the pseudo-second order equation with the calculated equilibrium adsorption capacity ($q_{e(cal)}$) shows the EB dye adsorption on PsLw carbon-iron oxide composite best follows pseudo-second order kinetics than the pseudo-first order kinetics.

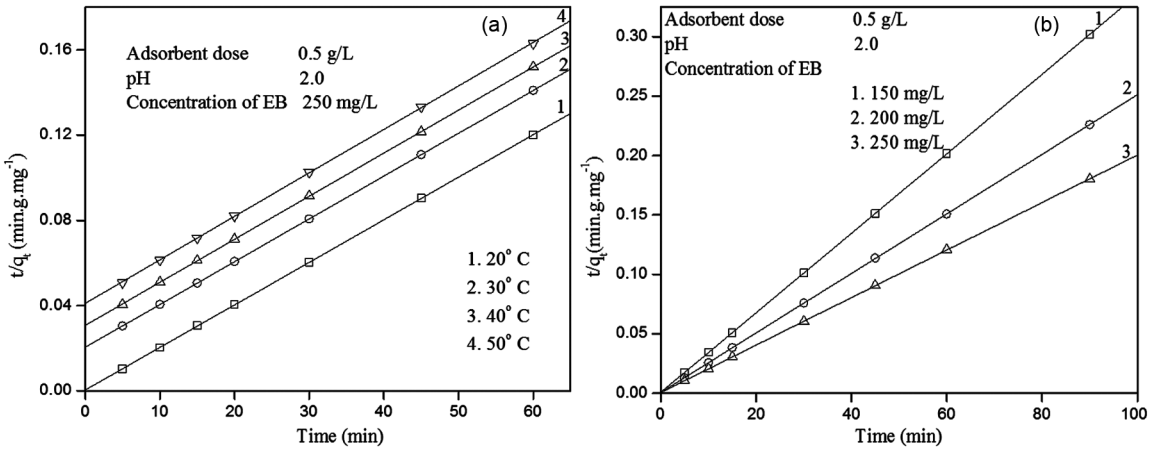

Fig. 6 — Pseudo-second order plot of EB dye onto PsLw carbon-iron oxide composite at different (a) concentrations and (b) temperatures.

Table 4 — Thermodynamic parameters

Temperature (K)	- ΔG° (KJ/mol)	-ΔH° (KJ/mol)	-ΔS° (J/mol k)
293	28.28	105.0	0.2626
303	24.76		
313	22.61		
323	20.89		

Thermodynamic parameters

Thermodynamic parameters such as free energy change (ΔG°), enthalpy change (ΔH°), and entropy change (ΔS°) are used to predict the nature of sorption process. The equilibrium constant (K_o) was determined using the method of Khan and Singh by plotting of $\ln q_e/C_e$ versus q_e and extrapolating to zero q_e. The free energy change (ΔG°), enthalpy change (ΔH°), and entropy change (ΔS°) for EB dye adsorption were determined at different temperatures using equations (8), (9) and (10).

$$\Delta G^o = -RT\ln K_o \quad \ldots(8)$$

$$\ln K = \left(\Delta S^o/R\right) - \left(\Delta H^o/RT\right) \quad \ldots(9)$$

$$\Delta G^\circ = \Delta H^\circ - T\Delta S^\circ \quad \ldots(10)$$

where, T is the temperature (K) and R is the gas constant (8.314 J/mol K). ΔH° and ΔS° can be calculated from the slope and the intercept of the plot of thermodynamic equilibrium constant (K) versus 1/T (Figure is not shown). The thermodynamic parameters are given in Table 4. The negative value of ΔG° and ΔH° indicate the EB dye uptake on PsLw carbon-iron oxide composite is spontaneous and exothermic in nature. The negative value of ΔS° shows the decreased randomness at the solid-solute interface during the adsorption process. PsLw carbon-iron oxide composite shows the possibility of some structural changes on the adsorbent surface which is evident from the IR and SEM studies. Thus the adsorption of EB dye on PsLw carbon-iron oxide composite is spontaneous, feasible and exothermic in nature[20,21].

Pore diffusion and mass transfer

In batch adsorption, pore size distribution plays a more important role than the surface area. To determine whether the intraparticle diffusion is the rate determining step or not, the data were analysed using Finkiam diffusion law[22] expressed by the following equation.

$$q = k_i t^{1/2} + c \quad \ldots(11)$$

where, k_i (mg/g/min$^{1/2}$) is the intraparticle diffusion constant and q is the amount adsorbed (mg/g) at time 't'. In many adsorption processes the adsorbate species transported from the bulk of the solution into the solid phase through an intraparticle diffusion process and it can be the rate-limiting step[23]. The plot of $t^{1/2}$ versus q was found to parabolic [Fig. 7(a)] yet linear for some contact time and moreover they do not pass through origin. The intraparticle diffusion constant, k_i is the slope of the linear portion of the plot and the k_i values obtained are given in Table 5 for the temperatures studied. The increase in k_i values with increase in temperature indicates the intraparticle diffusion becomes easier at higher temperature. This factor together with energetics thermodynamics of adsorption with positive ΔS° helps to understand the effect of temperature. The pore diffusion constant (k_i) at different temperatures are given in Table 5.

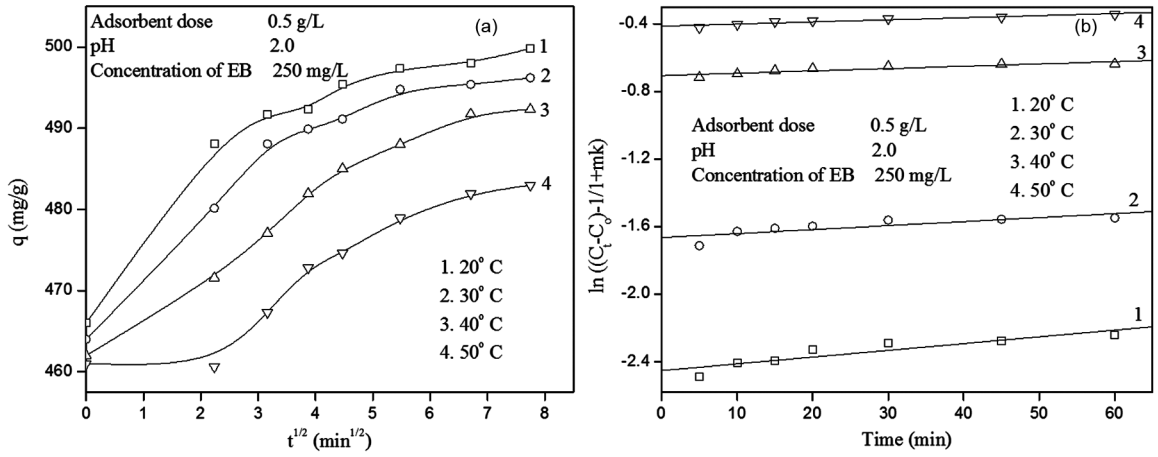

Fig. 7 — Plots of EB dye adsorption of (a) intra particle diffusion (b) mass transfer onto PsLwcarbon-iron oxide composite at different temperatures.

Table 5 — Pore diffusion and mass transfer coefficients

C_o (mg/L)	T (°C)	Intra particle diffusion (k_i) (mg/g/min$^{1/2}$)	$\beta_L \times 10^{-5}$
150	30	5.5413	-
200	30	5.8782	-
250	30	6.0925	-
250	20	3.0415	0.0118
250	30	4.8498	0.4388
250	40	6.0961	2.3334
250	50	6.4914	4.2463

Mckay *et al*., proposed a mathematical model to study the mass transfer and it was applied for the adsorption of EB dye onto the PsLw carbon-iron oxide composite which is defined by equation 12.

$$\ln(C_t/C_o - 1/1+mk) = [(1+mk/mk)\beta_L S_s]t + (mk/1+mk) \quad \ldots(12)$$

where C_o (mg/L) is the initial adsorbate concentration and C_t (mg/L) is the adsorbate concentration after time t, 'm' is the mass of adsorbent per unit volume of particle free solution (g/L), k (L/g) is the product of Langmuir constants Q_o and b, β_L (cm/s) is the mass transfer coefficient while S_s is the outer surface area of adsorbent per unit volume of particle free slurry (cm^{-1}). The values of 'm' and 'S_s' were calculated using the relations (13) and (14).

$$m = W / v \quad \ldots(13)$$

$$S_s = 6m/(1-\varepsilon_p)\, d_p\, \rho_p \quad \ldots(14)$$

where W is the weight of adsorbent (g), '**v' is** the volume of particle free adsorbate solution (L), d_p is the particle diameter (cm), ρ_p is the density of adsorbent (g/cm^3) and ε_p is the porosity of adsorbent particle. The plot of ln $[(C_t/C_o)-(1/1+mk)]$ against t is a straight line and is shown in Fig. 7(b). From the slope and intercept of the plot, the mass transfer coefficient β_L was calculated and are given in Table 5. The mass transfer coefficient increases with increase in temperature. This shows that mass transfer is also a part of the sorption process.

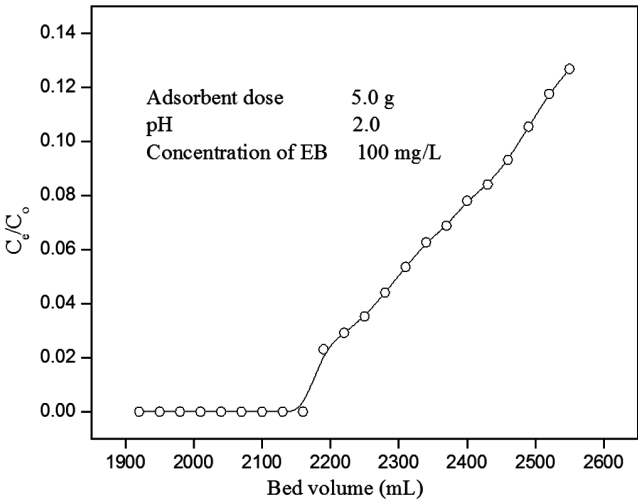

Fig. 8 — Breakthrough curve for adsorption of EB dye on PsLw carbon-iron oxide composite.

Column study

Column adsorption process is vital for industrial application and in the present study the column data was analysed using Thomas model[11,24].The observed data fit to the linearised form of the Thomas model (equation 6). The break through curve for the removal

Table 6 — Adsorption capacity of different adsorbents

Adsorbent	Adsorption capacity, q (mg/g)	References
Diatomite supported layered double hydroxide	625.2	25
Sawdust activated carbon impregnated with NaOH	100	26
Salt activated Raphiahookeri seeds	8.78	27
Spent/Fresh R. arrhizus biomass	355.87/363.64	28
Used cigarette filter ash	32.68	29
Lemon citrus peel active carbon	296	30
Terminalia Catappa Endocarp Activated Carbon	41.49	21
PsLw carbon	22.88	31
Crop waste pumpkin seed hulls	16.4	15
Mesoporous graphitic activated carbon of Bael tree	576.12	32
Erythrosine-imprinted magnetic chitosan	116.27	20
Poly(MMA-ethylene glycol dimethacrylate) copolymer	105.6	17
Montmorillonite	578.03	33
Principal activated carbon-Activated carbon	89.3	34
Sugarcane bagasse	500	35
Chitosan/ Chitin hydrogel SiO_2 hybrid materials	70.38/131.96	36
De-oiled mustard	3046.41	37
Hen feathers	15.43	38
Bottom ash/de-oiled soya	16.16/9.51	39
PsLw carbon-iron oxide composite	487.8	Present study

of EB is shown in Fig. 8. The flow rate is 3 mL/min for 100 mg/L initial concentration and 5 cm bed height was evaluated.

Effluent EB dye concentration was found to be zero for the first 72 bed volumes. After 72 bed volumes, the retention of EB dye by the column gradually decreases as the bed volume increases. A plot of log (C_o/C_e-1) versus V was made to compute the values of Thomas rate constant 'K' (K = 0.0636 mL/min/mg) and 'q_o' (q_o = 14.64 mg/g) the maximum solid phase concentration were determined from the slope and the intercept respectively. When the column was saturated with EB dye, it was eluted with 0.1 M NaOH and washed with deionised water and used for further cycles.

Desorption studies

In order to recover the adsorbed EB dye and regenerate the adsorbent, desorption was carried out with 0.1 M NaOH. It was observed that desorption of EB dye was 92% in the first cycle, 86% and 84% in the second and third adsorbed-desorbed cycle respectively.

Comparison with other adsorbents

A comparative report of adsorption capacity of various adsorbents reported for the removal of EB dye is given in Table 6. It shows that PsLw carbon-iron oxide composite has comparable adsorption capacity with other adsorbents.

Conclusion

The results of the present investigation depict that the removal of EB dye is highly *p*H dependent and the maximum adsorption occurs at *p*H = 2.0. The equilibrium was attained within 60 min of contact time and the sorption process is more rapid because the surface of PsLw carbon-iron oxide composite has more active sites for adsorbate molecules. The adsorption efficiency increases with an increase in the initial concentration and contact time. The removal of EB dye decreases with increasing temperature. The EB dye uptake of PsLw carbon-iron oxide composite fits to Langmuir isotherm with maximum adsorption efficiency 487.8 mg/g at 20°C. The kinetic studies of sorption process follow pseudo-second order kinetics. Thermodynamic parameters exhibit the adsorption process is spontaneous, feasible and exothermic in nature. The column analysis is helpful to apply this process at industrial level. SEM and FTIR spectroscopic studies show that the uptake of EB is due to electrostatic interaction between the dye and the adsorbent. Pore diffusion and mass transfer studies show that they are also part of the adsorption process. Therefore PsLw carbon-iron oxide composite could be used as a potential adsorbent for the removal of hazardous dyes from aqueous systems.

Acknowledgements

The authors acknowledge the administration of Sri K.G.S Arts College, Srivaikuntam, St. Xavier's

College (Autonomous), Palayamkottai and Rani Anna Government College for Women, Tirunelveli for all the laboratory studies.

References

1 Uysal O K & Aral E, *Turk J Med Sci*, 28 (1998) 363.
2 Oliveria L C A, Rios R V R A, Fabris J D, Garg V, Sapag K & Lago R M*, Carbon*, 40 (2002) 2177.
3 Dankova Z, Mockovciakova A & Orolinovo M, *Energy Environ Eng*, 1 (2013) 74.
4 Zhang H L, Li, XC, He, G H, Zhan J J & Liu D, *Ind Eng Chem Res*, 52 (2013) 16902.
5 Yao S, Liu Z & Shi Z, *J Environ Health Sci Eng*, 12 (2014) 58.
6 Schwarz J A, Driscoll C T & Bharot A K, *J Colloid Interf Sci*, 97 (1984) 55.
7 Chang Q, Lin W & Ying W C, *J Hazard Mater,* 184 (2010) 515.
8 Palit D & Moulik S P, *Indian J Chem*, 39A (2000) 611.
9 Adamson A W, *Physical chemistry of Surfaces*, 5thedn, (John wiely & Sons, Inc, New York, USA) (1990) 435.
10 Potgiefer J H, *J Chem Edu*, 68 (1991) 349.
11 Thomas H C, *Ann NY Acad Sci*, 49 (1948) 161.
12 Reynolds T D & Richards P A, *Unit operations and processes in Environmental Engineering*, PWS Boston, USA*,* (1996) 142.
13 Pan X & Zhang D*, Electron J Biotechnol*, 12 (2009) 1
14 Ansari R & Mosayebzadeh Z, *Iran Polym J*, 19 (2010) 541.
15 Apostol L C, Ghinea C, Alves M & Gavrilescu M, *Desalin Water Treat*, 57 (2015) 22585.
16 Zeyada H M, El-Mallah H M, Atwee T & El-Damhogi D G, *Spectrochim Acta A Mol Biomol Spectrosco*, 179 (2017) 120.
17 Altindag I G, Dincer A, Becerik S, Eser A & Aydemir T, *Desalin Water Treat*, 54 (2014) 1717.
18 Lagergren S, *Handlingar*, 24 (1898) 1.
19 Okey-Onyesolu C F, Onukwuli O D, Ejimofor M I & Okoye C C, *Heliyon*, 6 (2020) 1.
20 Eser A, Aydemir T, Becerik S & Dincer A, *Desalin Water Treat*, 57 (2015) 17002.
21 Okoye C C, Onukwuli O D, Okey-Onyesolu C F & Nwokedi I C, *Chem Process Eng Res*, 43 (2016) 26.
22 Chang M Y & Juang R S, *J Colloid Interf Sci*, 278 (2004) 18.
23 Semerjian L, *J Hazard Mater*, 173 (2010) 236.
24 Mckay G, Otterburn M S & Sweeney A G, *Water Res*, 15 (1981) 327.
25 Shamsayei M, Yamini Y & Asiabi H, *Int J Environ Anal Chem*, (2020) 1.
26 Benhabiles S & Rida K, *Part Sci Technol*, (2020) 237.
27 Okoye C C, Onukwuli O D & Okey-Onyesolu C F, *J King Saud Univ Sci*, 31 (2019) 849.
28 Salvi N A, *Appl Water Sci*, 8 (2018) 205.
29 Ajoor M & Moeinpour F, *J Phys Theor Chem IAU Iran*, 14 (2017) 81.
30 Sharifzade G, Asghari A & Rajabi M, *R Soc Chem Adv*, 7 (2017) 5362.
31 Rani J M, Murugan M, Subramaniam P & Subramanian E, *Indian J Chem Technol*, 23 (2016) 22.
32 Valliammai S, Subbareddy Y, Nagaraja K S & Jeyaraj B, *J Mater Environ Sci*, 6 (2015) 2836.
33 Kaur M & Datta M, *Sep Sci Technol*, 48 (2013) 1370.
34 Al-Degs Y S, Abu-El-Halawa R & Abu-Alrub S S, *Chem Eng J*, 191 (2012) 185.
35 Sharma P & Kaur H, *Appl Water Sci*, 1 (2011) 135.
36 Copello G J, Mebert A M, Raineri M, Pesenti M P & Diaz L E, *J Hazard Mater*, 186 (2011) 932.
37 Jain R & Sikarwar S, *J Hazard Mater*, 164 (2009) 627.
38 Gupta V K, Mittal A, Kurup L & Mittal J, *J Colloid Interf Sci*, 304 (2006) 52.
39 Mittal A, Mittal J, Kurup L & Singh A K, *J Hazard Mater B*, 138 (2006) 95.